

We are IntechOpen, the world's leading publisher of Open Access books Built by scientists, for scientists

6,900

Open access books available

185,000

International authors and editors

200M

Downloads

Our authors are among the

154

Countries delivered to

TOP 1%

most cited scientists

12.2%

Contributors from top 500 universities



WEB OF SCIENCE™

Selection of our books indexed in the Book Citation Index
in Web of Science™ Core Collection (BKCI)

Interested in publishing with us?
Contact book.department@intechopen.com

Numbers displayed above are based on latest data collected.
For more information visit www.intechopen.com



Sensitivity and Uncertainty Quantification of Neutronic Integral Data Using ENDF/B-VII.1 and JENDL-4.0 Evaluations

Mustapha Makhloul, H. Boukhal, T. El Bardouni, E. Chakir, M. Kaddour and S. Elouahdani

Abstract

Many integral neutronic parameters such as the effective multiplication factors (k_{eff}) are based on neutron reactions with matter through cross sections. However, these cross sections present uncertainties, of origin multiple, which reduce the safety margin of nuclear installations. In order to minimize these risks, a sensitivity analysis is necessary to indicate the rate of change of a reactor performance parameter compared to variations in cross sections. Thus, several critical benchmarks were taken from the International Handbook of Evaluated Criticality Safety Benchmark Experiments (IHECSBE), and their sensitivities and covariance matrix of the desired cross section were processed by MCNP6 and NJOY codes, respectively, in ENDF/B-VII.1 and JENDL-4.0 evaluations. The results obtained show that the 44 energy groups give the most varied sensitivity profiles than those given by others (15 and 33). In addition, we observed large uncertainties on the k_{eff} due to the H-1 and O-16 cross-sectional uncertainties ($\sim 200\text{--}1000$ pcm) in ENDF/B -VII.1 and the U-235 cross section in JENDL-4.0; however, k_{eff} 's uncertainties due to the cross-sectional uncertainties of the U-238 are very small.

Keywords: k_{eff} , sensitivity, covariance matrix, uncertainty, MCNP6.1, NJOY, multigroup cross section

1. Introduction

Prediction of integral nuclear parameters requires a reliable nuclear database such as microscopic nuclear parameters, cross sections, covariance matrices, etc. Many previous works [1, 2] have proved that the capture cross section of the uranium 235 has an important effect on the criticality calculations [3, 4]. For example, the relative uncertainty of k_{eff} in BFS core due to the ^{235}U capture cross-sectional uncertainty is near 202 pcm [5].

In present study, the uncertainty prediction in the multiplication factors is based on the ENDF/B-VII.1 and JENDL-4.0 evaluations where MCNP6 [6] Monte Carlo code is used for the sensitivity and k_{eff} calculations and the NJOY99 [7] is applied to calculate the covariances in three energy group structures (15, 33 and 44) for the

most abundant isotopes in the studied benchmarks (^{235}U , ^{238}U , ^1H , and ^{16}O). All benchmarks were taken from IHECSBE [8].

2. Study approach

2.1 Multigroup structure

In this article, the effect of the multigroup energy of neutrons on the sensitivity of multiplication factors was studied for three cases (15, 33, and 44 groups). The covariances for many cross sections are often presented in the evaluated data libraries (ENDF/B-VII.1 and JENDL-4.0). All files were processed by the NJOY99 code to calculate the multigroup of interest cross sections in the ENDF-6 format. The modules RECONR and BROADR were used before to reconstruct the cross sections (MF = 3) at room temperature 300°K. The GROUPT module was used to generate the desired data in the grouped-wise format gendf for the three presentations (15, 33, and 44 groups) to retain the characteristic structure in the cross sections between 10^{-5} eV and 20 MeV. The energetic structures were generated from the fine-group library for resonance nuclides, with different weight flux functions: fission Maxwellian (10 MeV–70 keV), 1/E (70 keV–0.125 eV), and thermal Maxwellian (0.125– 10^{-5} eV). **Tables 1–3** below present the three energy group structures.

Figures below illustrate the comparison of the pointwise and multigroup representations for the $^{235,238}\text{U}$ cross sections (**Figures 1 and 2**).

Figures above present that the pointwise and multigroup cross sections are very close in the two evaluations ENDF/B-VII.1 and JENDL-4.0.

2.2 Covariance data of cross sections

It is necessary to process the multigroup covariance matrices for each energy group structure (15, 33, and 44). Thus, an appropriate input file for nuclear code NJOY was prepared using several modules as ERROR, GROUPT, and COVR [11–13] to process the ENDF file (MF = 33) and generate the multigroup covariance matrices for the desired cross sections. The following figures show a comparison of these covariance matrices in the two evaluations studied using the structures of 15, 33, and 44 energy groups.

Figure 3 shows the uncertainty and covariance for the ^{235}U elastic cross section in the energy region from 10^{-5} eV to 20 MeV. In this figure, we can see that the

Group number	Energy range (eV)	Group number	Energy range (eV)
1	1.0000E-05	9	2.4800E+04
2	1.1000E-01	10	6.7400E+04
3	5.4000E-01	11	1.8300E+05
4	4.0000E+00	12	4.9800E+05
5	2.2600E+01	13	1.3500E+06
6	4.5400E+02	14	2.2300E+06
7	2.0400E+03	15	6.0700E+06
8	9.1200E+03	16	1.9600E+07

Table 1.
15 Neutron energy group structure [9].

Group number	Upper energy (eV)	Group number	Upper energy (eV)	Group number	Upper energy (eV)
1	1.0000E-01	12	4.5400E+02	23	1.1100E+05
2	5.4000E-01	13	7.4900E+02	24	1.8300E+05
3	4.0000E+00	14	1.2300E+03	25	3.0200E+05
4	8.3200E+00	15	2.0300E+03	26	4.9800E+05
5	1.3700E+01	16	3.3500E+03	27	8.2100E+05
6	2.2600E+01	17	5.5300E+03	28	1.3500E+06
7	4.0200E+01	18	9.1200E+03	29	2.2300E+06
8	6.7900E+01	19	1.5000E+04	30	3.6800E+06
9	9.1700E+01	20	2.4800E+04	31	6.0700E+06
10	1.4900E+02	21	4.0900E+04	32	1.0000E+07

Table 2.
33 Neutron energy group structure [10].

Group number	Upper energy (eV)	Group number	Upper energy (eV)	Group number	Upper energy (eV)
1	1.0000E-05	16	3.2500E-01	31	3.0000E+03
2	3.0000E-03	17	3.5000E-01	32	1.7000E+04
3	7.5000E-03	18	3.7500E-01	33	2.5000E+04
4	1.0000E-02	19	4.0000E-01	34	1.0000E+05
5	2.5300E-02	20	6.2500E-01	35	4.0000E+05
6	3.0000E-02	21	1.0000E+00	36	9.0000E+05
7	4.0000E-02	22	1.7700E+00	37	1.4000E+06
8	5.0000E-02	23	3.0000E+00	38	1.8500E+06
9	7.0000E-02	24	4.7500E+00	39	2.3540E+06
10	1.0000E-01	25	6.0000E+00	40	2.4790E+06
11	1.5000E-01	26	8.1000E+00	41	3.0000E+06
12	2.0000E-01	27	1.0000E+01	42	4.8000E+06
13	2.2500E-01	28	3.0000E+01	43	6.4340E+06
14	2.5000E-01	29	1.0000E+02	44	8.1873E+06
15	2.7500E-01	30	5.5000E+02	45	2.0000E+07

Table 3.
44 Neutron energy group structure [10].

lowest uncertainty is given by the 44-group structure where around the energy 10 keV, the uncertainty is ~4% in the ENDF/B-VII.1 and ~ 9.5% in JENDL-4.0. In addition, negative correlations are observed in JENDL-4.0.

According to **Figure 4**, the maximum uncertainties in the fission cross sections of the ²³⁵U in the energy less than 10 eV are, respectively, ~7.5% and ~1% in JENDL-4.0 and ENDF/B-VII.1 for 15 and 33 groups; however, in the 44-group structure, one can see that this maximum is ~15% around the energy 3 eV. In the energy interval [10 eV; 20 MeV], these uncertainties are very close to 1% for the two evaluations in 33- and 44-group structures, while for the 15-group structure,

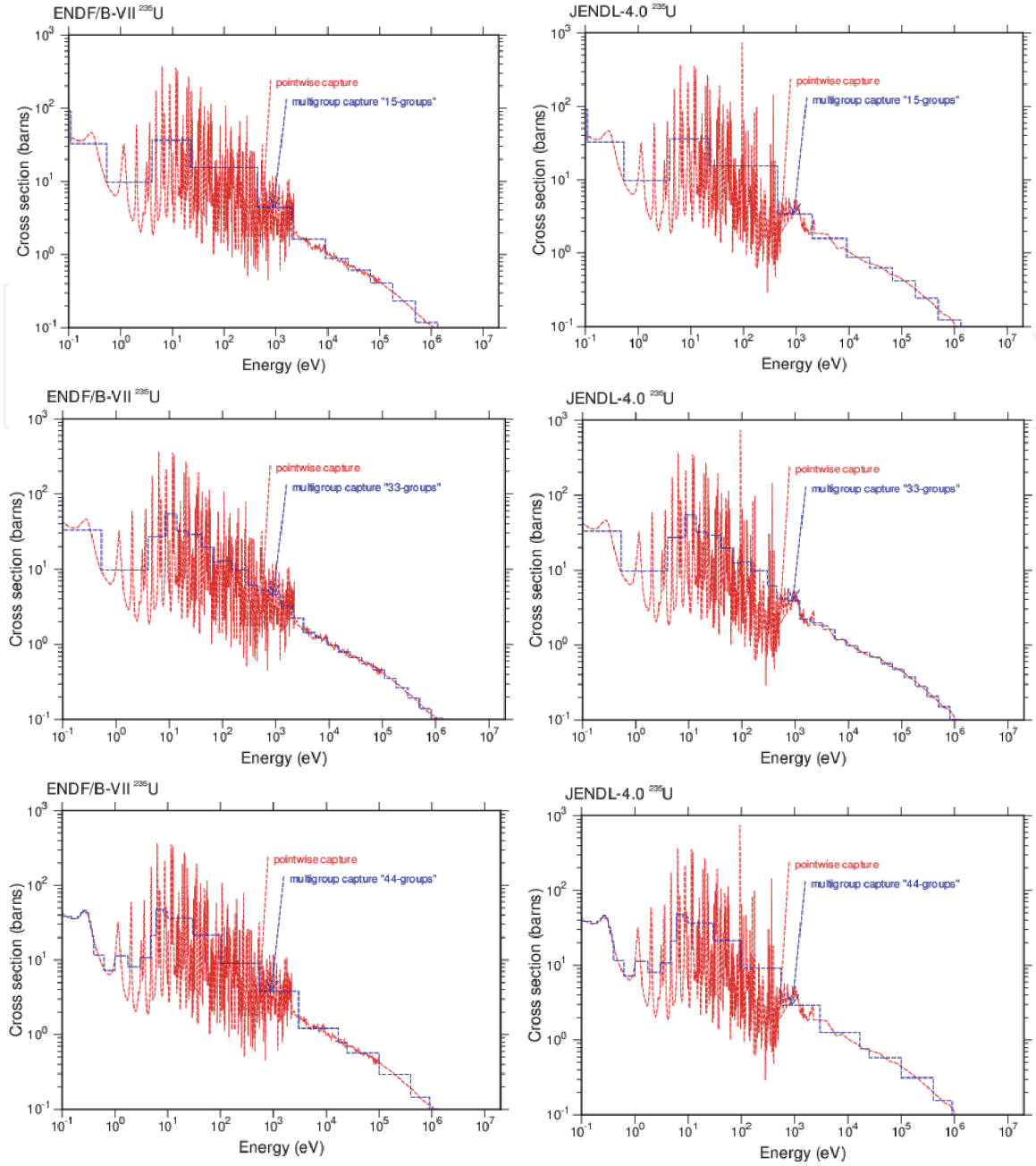


Figure 1.
The pointwise and multigroup (15, 33, and 44) capture cross section for the ^{235}U .

the uncertainties in JENDL-4.0 are higher than those in ENDF/B-VII.1. Also, negative correlations appeared in JENDL-4.0.

2.3 Sensitivity-uncertainty theory

Sensitivity coefficients represent the percentage effect on some nuclear system response (e.g., multiplication factor k_{eff}) due to a percentage change in an input parameter such as cross section (capture, fission, elastic, inelastic, etc.). The sensitivity of k_{eff} (noted simply k) to a multigroup cross section $\sigma_{x,g}$, for an energy group g , is defined according to [14] by Eq. (1), where the first order of the perturbation theory is used [15–17]:

$$S_{x,g} = \frac{\sigma_{x,g}}{k} \frac{\partial k}{\partial \sigma_{x,g}} \quad (1)$$

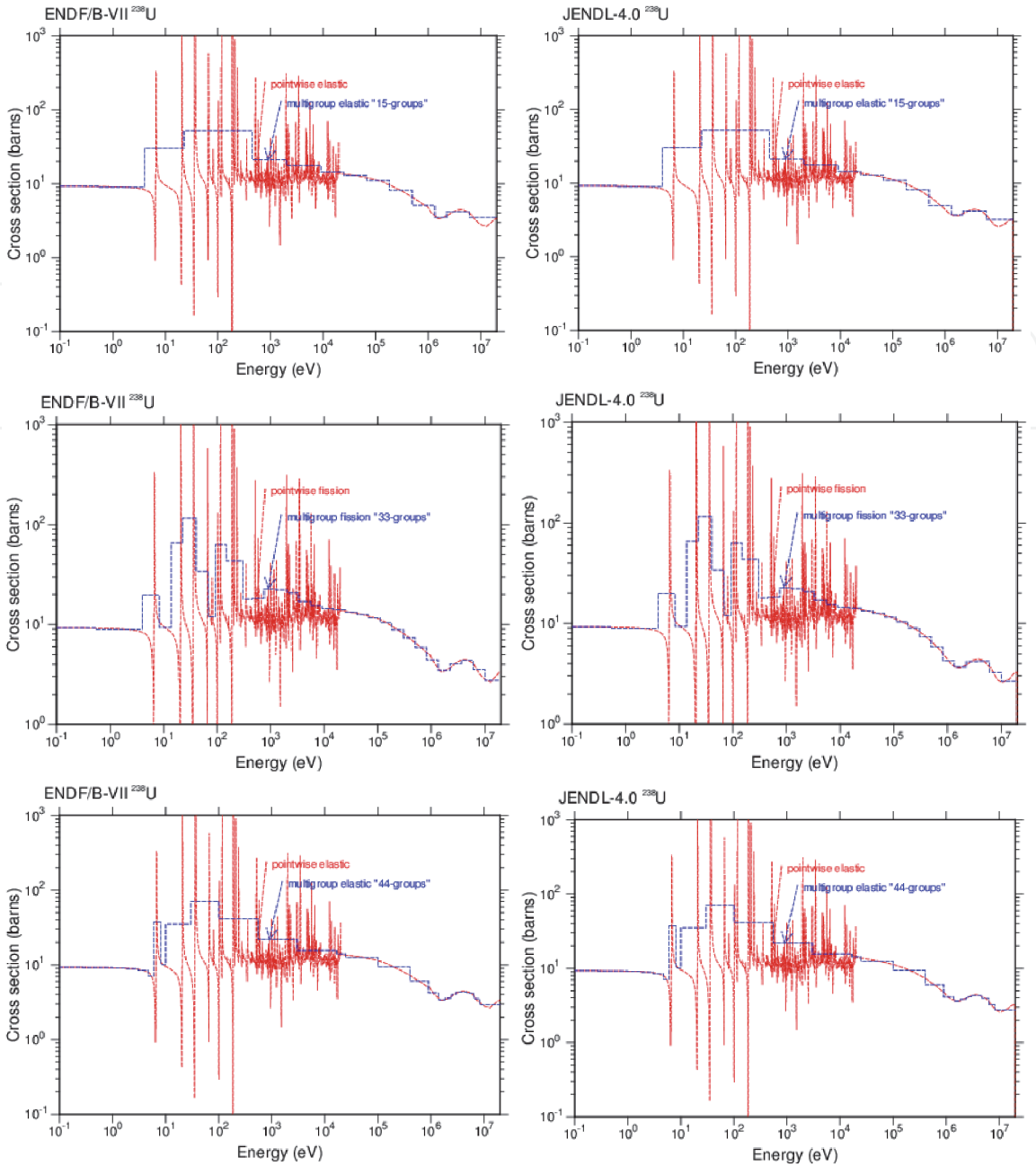


Figure 2.
 The pointwise and multigroup (15, 33, and 44) elastic cross section for the ^{238}U .

These coefficients are supposed to be constant in the first order of perturbation theory, so the sensitivity matrix S (Eq. (2)) is also constant [18–20]:

$$S_k = \left[\frac{\sigma_i}{k_j} \frac{\partial k_j}{\partial \sigma_i} \right] \quad i = 1.2. \dots .n \text{ and } j = 1.2. \dots .m \tag{2}$$

where m is the number of critical systems considered and n is the number of energy groups ($n = 15, 33, \text{ and } 44$).

The sensitivity matrix coefficients have been calculated using MCNP6.1 code using KSEN card.

The integral quantities calculated with a reference cross section set σ are denoted by k . The integral quantities k' calculated with a cross section set σ' , which deviates by $\delta\sigma$ from σ , have the following relation with k :

$$k' = k(1 + S.\delta\sigma) \tag{3}$$

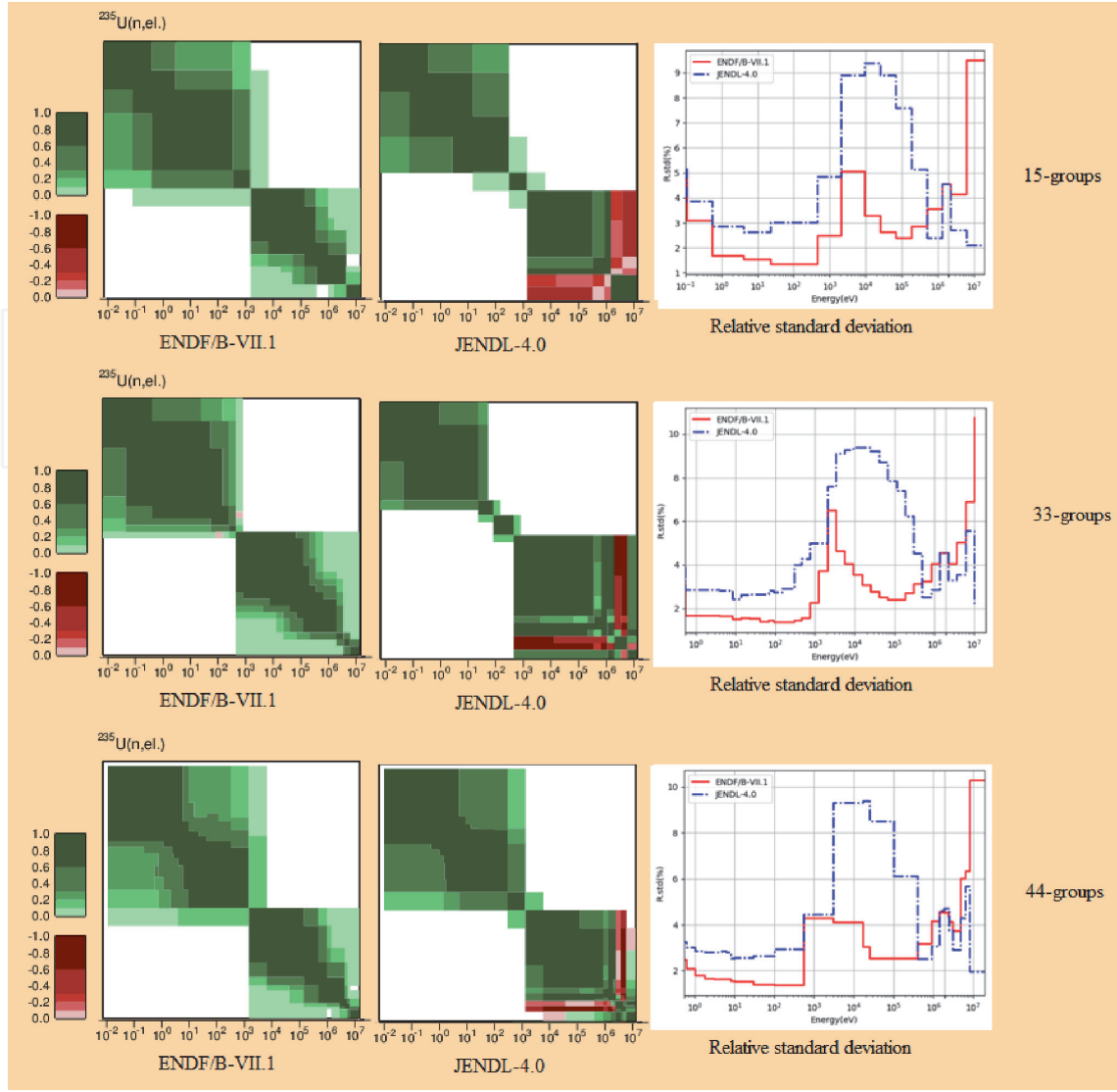


Figure 3. Uncertainty and covariance for the ^{235}U elastic cross section using 15, 33, and 44 structure energy groups in ENDF/B-VII.1 and JENDL-4.0 evaluations.

The covariance of k'/k is given by

$$\begin{aligned} V_k &= (S\sigma' - S\sigma)(S\sigma' - S\sigma)^t \\ V_k &= S(T - T_0)(T - T_0)^t S^t \\ V_k &= SMS^t \end{aligned} \quad (4)$$

where t stands for the transpose of the matrix S .

The square root of the diagonal term V_{ii} of V_k is the standard deviation in the integral quantity k_i . Thus, the prior nuclear data uncertainty of k can be obtained in matrix expression form by the so-called sandwich rule [20, 21]:

$$(\Delta k)^2 = SMS^t \quad (5)$$

The non-diagonal term V_{ij} ($i \neq j$) gives the degree of correlation between the errors of k_i and k_j . The element r_{ij} of the correlation matrix is obtained by dividing the element V_{ij} by the products of standard deviation V_{ii} and V_{jj} :

$$r_{ij} = \frac{V_{ij}}{\sqrt{V_{ii}V_{jj}}} \quad (6)$$

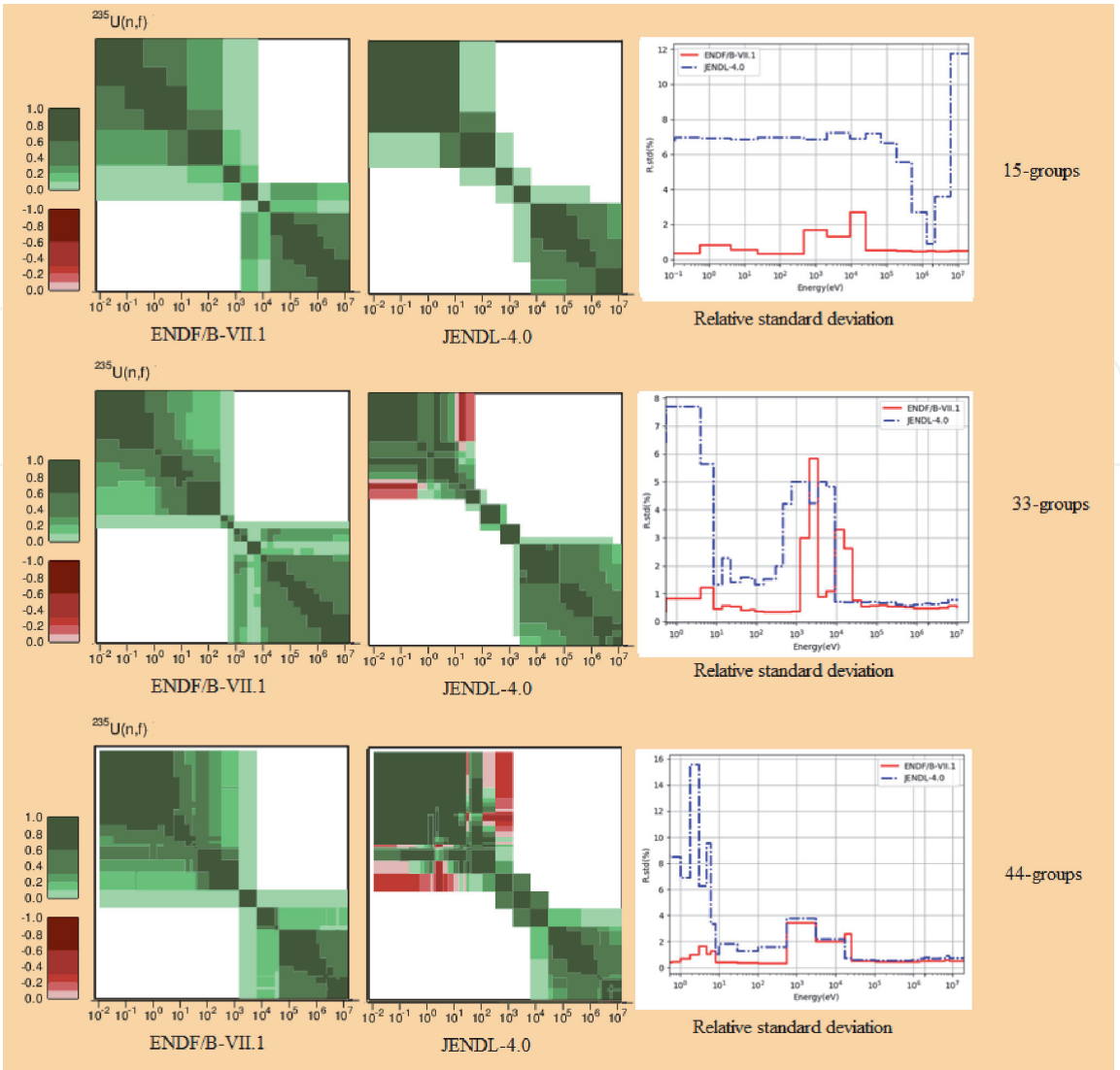


Figure 4. Uncertainty and covariance for the ^{235}U fission cross section using 15, 33, and 44 energy group structures in ENDF/B-VII.1 and JENDL-4.0 evaluations.

A common practice in uncertainty calculations is the relative sensitivity coefficients provided from the sensitivity analysis. Therefore, the relative matrices are used as

$$(\Delta k/k)^2 = GPG^t \tag{7}$$

where G is the relative sensitivity matrix and P is the relative covariance matrix of the interest cross section.

Eq. (7) mathematically links the uncertainty of the integral data and the uncertainties of the cross sections through the associated sensitivity coefficients. Thus, a high sensitivity and an uncertain cross section generate a large uncertainty in k.

3. Results and discussion

3.1 Description of benchmark systems

In this work, 25 HEU-SOL-THERM thermal experiments, 4 HEU-MET-INTER intermediate experiments, and 21 HEU-MET-FAST fast experiments are studied. The calculated, experimental k_{eff} and their uncertainties for each benchmark are

Benchmarks	k.exp	std.exp	k.cal (ENDF/B-VII.1)	std.cal	k.cal (JENDL-4.0)	std.cal
Hst001.001	1.0004	0.0060	0.99815	0.00005	0.99952	0.00005
Hst001.002	1.0021	0.0072	0.99722	0.00006	0.99927	0.00006
Hst001.003	1.0003	0.0035	1.00155	0.00005	1.00296	0.00005
Hst001.004	1.0008	0.0053	0.99815	0.00005	1.00048	0.00005
Hst001.005	1.0001	0.0049	0.99874	0.00005	0.99949	0.00005
Hst001.006	1.0002	0.0046	1.00196	0.00005	1.00283	0.00005
Hst001.007	1.0008	0.0040	0.99781	0.00005	0.99910	0.00005
Hst001.008	0.9998	0.0038	0.99797	0.00005	0.99930	0.00005
Hst001.009	1.0008	0.0054	0.99412	0.00006	0.99633	0.00006
Hst001.010	0.9993	0.0054	0.99241	0.00005	0.99338	0.00005
Hst009.001	0.9990	0.0043	0.99695	0.00005	1.00096	0.00005
Hst009.002	1.0000	0.0039	0.99686	0.00005	1.00034	0.00005
Hst009.003	1.0000	0.0036	0.99556	0.00005	0.99830	0.00005
Hst009.004	0.9986	0.0035	0.98894	0.00005	0.99112	0.00005
Hst009.010	1.0000	0.0057	0.99745	0.00005	1.00153	0.00005
Hst010.001	1.0000	0.0029	0.99453	0.00005	0.99633	0.00005
Hst010.002	1.0000	0.0018	0.99496	0.00005	0.99678	0.00005
Hst010.003	1.0000	0.0029	0.99247	0.00005	0.99237	0.00005
Hst010.004	0.9992	0.0029	0.99052	0.00005	0.99994	0.00004
Hst011.001	1.0000	0.0023	0.99859	0.00004	0.99773	0.00003
Hst011.002	1.0000	0.0023	0.99866	0.00004	0.99602	0.00004
Hst012.001	0.9999	0.0058	0.99723	0.00003	0.99745	0.00004
Hst013.001	1.0012	0.0026	0.99868	0.00003	1.00569	0.00005
Hst028.001	1.0000	0.0023	0.99642	0.00005	0.99580	0.00004
Hst035.007	1.0000	0.0035	1.00467	0.00005	0.99938	0.00004
Hmi006.001	0.9977	0.0008	0.99297	0.00004	1.00151	0.00004
Hmi006.002	1.0001	0.0008	0.99682	0.00004	1.00315	0.00004
Hmi006.003	1.0015	0.0009	1.00082	0.00004	0.99751	0.00003
Hmi006.004	1.0016	0.0008	1.00732	0.00004	0.99025	0.00003
Hmf001.001	1.0004	0.0024	0.99976	0.00003	0.98929	0.00003
Hmf003.001	1.0000	0.0050	0.99501	0.00003	0.99386	0.00003
Hmf003.002	1.0000	0.0050	0.99436	0.00003	0.99208	0.00003
Hmf003.003	1.0000	0.0050	0.99918	0.00003	0.99638	0.00003
Hmf003.004	1.0000	0.0050	0.99721	0.00003	1.00187	0.00003
Hmf003.005	1.0000	0.0030	1.00146	0.00003	1.00190	0.00003
Hmf003.008	1.0000	0.0030	1.00214	0.00003	1.00515	0.00003
Hmf003.009	1.0000	0.0050	1.00244	0.00003	1.00960	0.00003
hmf003.010	1.0000	0.0050	1.00505	0.00003	0.99315	0.00003
Hmf003.011	1.0000	0.0030	1.00886	0.00003	0.99656	0.00004
Hmf008.001	0.9989	0.0016	0.99577	0.00003	0.99518	0.00003

Benchmarks	k.exp	std.exp	k.cal (ENDF/B-VII.1)	std.cal	k.cal (JENDL-4.0)	std.cal
Hmf011.001	0.9989	0.0015	0.99887	0.00004	0.99265	0.00003
Hmf012.001	0.9992	0.0018	0.99810	0.00003	0.99236	0.00003
Hmf014.001	0.9989	0.0017	0.99774	0.00003	0.99684	0.00003
Hmf015.001	0.9996	0.0017	0.99447	0.00003	0.99774	0.00003
Hmf018.002	1.0000	0.0014	0.99946	0.00003	0.99337	0.00003
Hmf020.002	1.0000	0.0028	1.00057	0.00003	0.99416	0.00003
Hmf021.002	1.0000	0.0024	0.99750	0.00003	1.00132	0.00004
Hmf022.002	1.0000	0.0021	0.99746	0.00003	0.99782	0.00003
Hmf026.011	0.9982	0.0042	1.00312	0.00004	1.00647	0.00005
Hmf028.001	1.0000	0.0030	1.00286	0.00003	1.00745	0.00005

Table 4.
K_{eff} benchmark cases and their statistical uncertainties (1σ).

	Hst001.001		Hst001.006		Hst035.007	
Isotope	ENDF/B-VII.1	JENDL-4.0	ENDF/B-VII.1	JENDL-4.0	ENDF/B-VII.1	JENDL-4.0
U-234	-2.7926E-03	-2.6083E-03	-2.0123E-03	-1.8550E-03	-2.3645E-03	-2.4621E-03
U-235	1.0503E-01	1.1931E-01	2.2592E-01	2.2535E-01	1.3115E-01	1.3959E-01
U-236	-2.9683E-04	-4.2700E-04	-5.0385E-05	-1.6201E-04	-2.3107E-04	-2.4627E-04
U-238	-2.7572E-03	-3.3237E-03	-1.1858E-03	-1.3662E-03	-6.4877E-03	-5.4229E-03
H-1	5.5723E-01	5.4111E-01	3.4059E-01	3.4260E-01	3.9636E-01	4.0646E-01
O-16	1.3385E-01	1.3190E-01	1.1264E-01	1.1672E-01	9.0869E-02	9.3703E-02
N-14	-2.8936E-03	-6.3375E-04	-2.9080E-03	-5.5300E-03	-3.6365E-03	-5.4211E-03

Table 5.
Total integrated sensitivity for thermal benchmark (%%).

Hmf001.001			Hmf003.001	
Isotope	ENDF/B-VII.1	JENDL-4.0	ENDF/B-VII.1	JENDL-4.0
U-234	5.1587E-03	7.4997E-03	1.4957E-03	1.9720E-03
U-235	8.0536E-01	8.0423E-01	1.4577E-01	1.5009E-01
U-238	1.7438E-02	1.7762E-02	4.2719E-02	4.1731E-02

Table 6.
Total integrated sensitivity for fast benchmark (%%).

summarized in **Table 4**. All calculations were performed using 100,000 neutrons per cycle, 150 inactive cycles, and 4000 active cycles to minimize statistical uncertainty (~5 pcm).

3.2 Total sensitivity evaluation

The total sensitivity calculations were performed in order to identify the most important cross sections for neutron-induced reactions in critical experiments summarized in **Table 4**. The total integrated sensitivities obtained using the ENDF/B-VII.1 and JENDL-4.0 evaluations are presented in **Tables 5** and **6**. We can see from

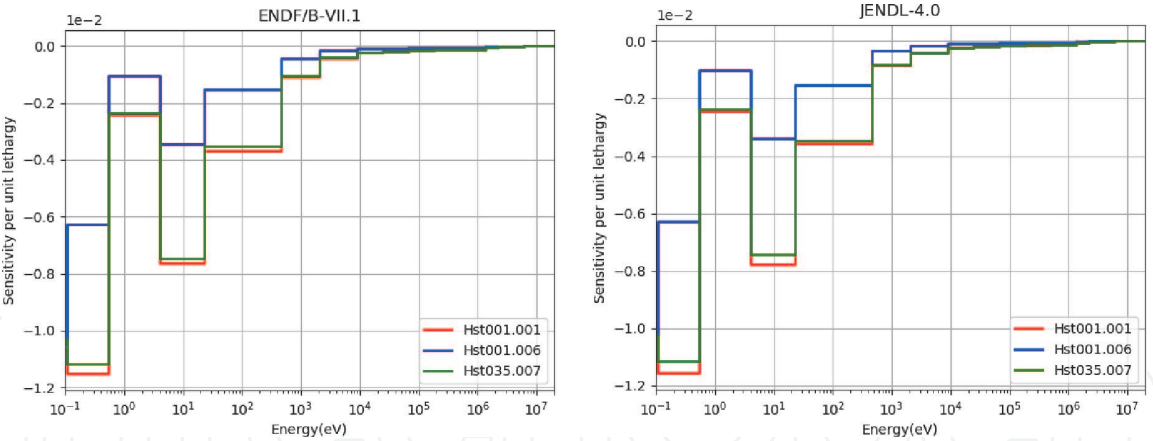


Figure 5.
Sensitivity profiles of ^{235}U capture cross section for thermal benchmarks with 15 energy groups—ENDF/B-VII.1 and JENDL-4.0.

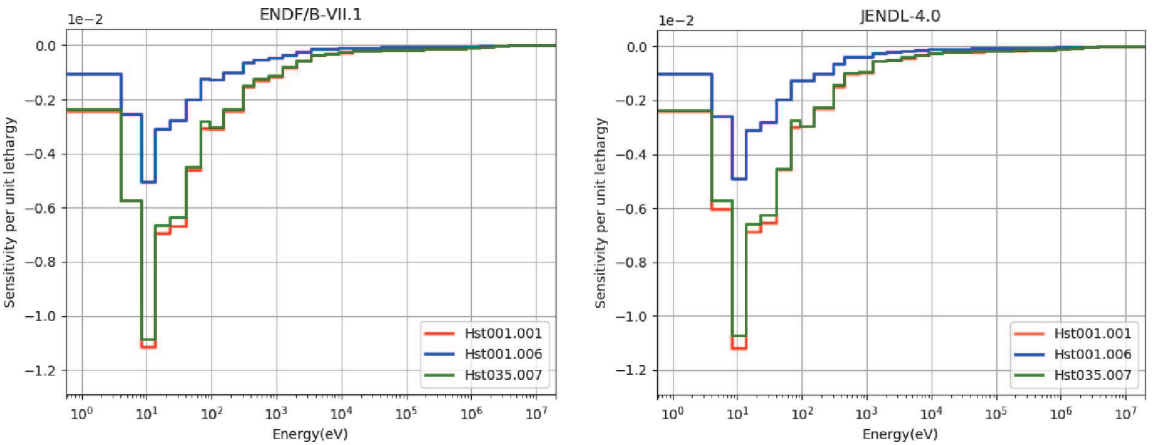


Figure 6.
Sensitivity profiles of ^{235}U capture cross section for thermal benchmarks with 33 energy groups—ENDF/B-VII.1 and JENDL-4.0.

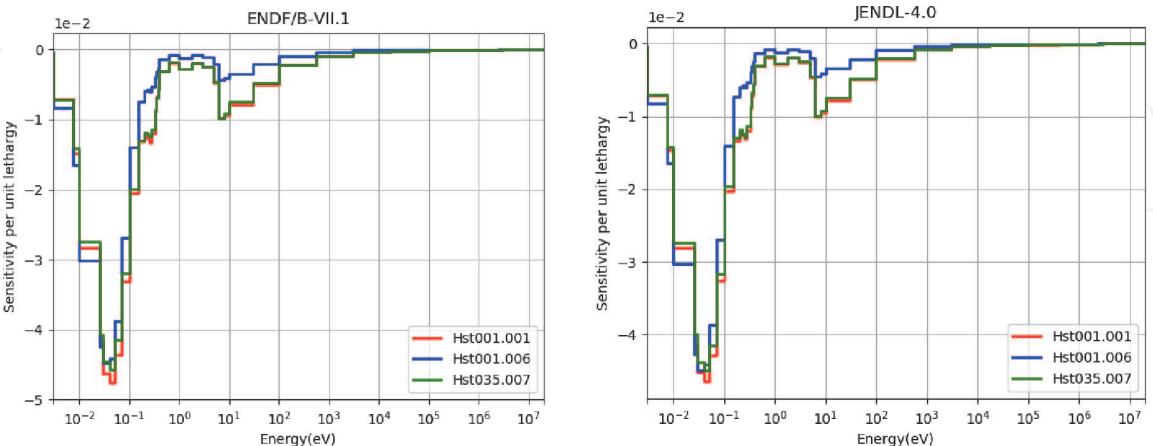


Figure 7.
Sensitivity profiles of ^{235}U capture cross section for thermal benchmarks with 44 energy groups—ENDF/B-VII.1 and JENDL-4.0.

these tables that the total integrated sensitivity obtained with the two nuclear evaluations is almost the same; in addition, the sensitivities of U-234, U-236, and N-14 are very low compared to the others. Thus, for the quantification of sensitivity and uncertainty, only U-235, U-238, H-1, and O-16 are taken into account.

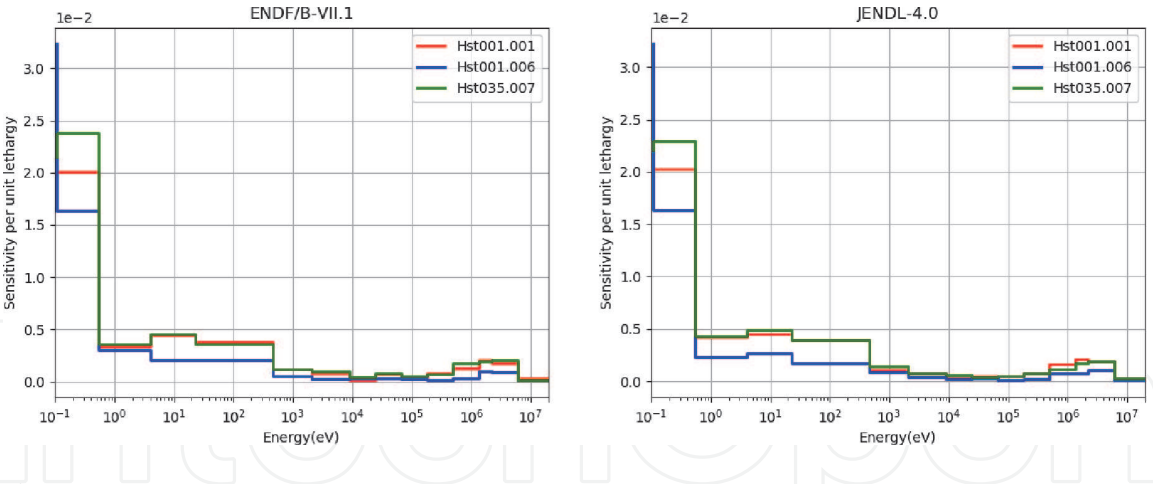


Figure 8.
Sensitivity profiles of ^{235}U fission cross section for thermal benchmarks with 15 energy groups—ENDF/B-VII.1 and JENDL-4.0.

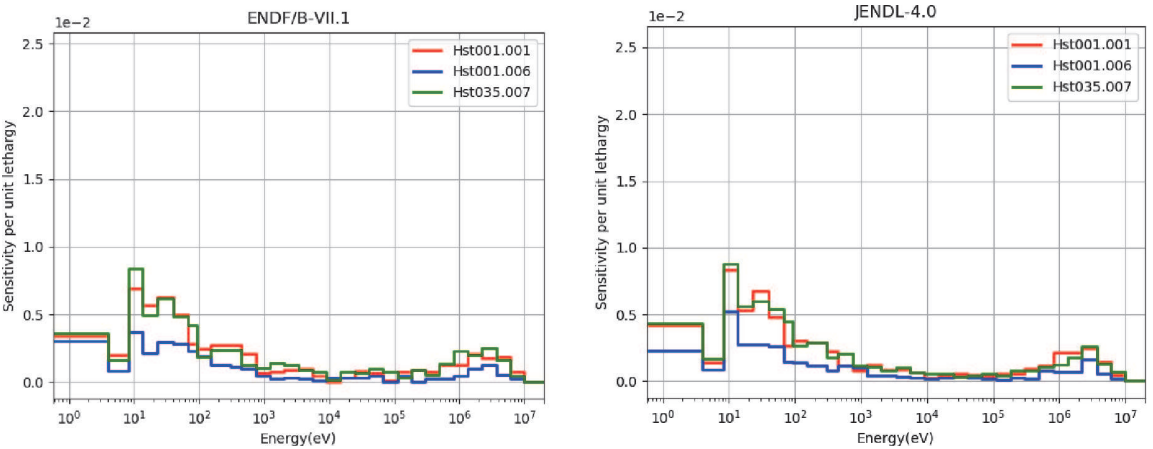


Figure 9.
Sensitivity profiles of ^{235}U fission cross section for thermal benchmarks with 33 energy groups—ENDF/B-VII.1 and JENDL-4.0.

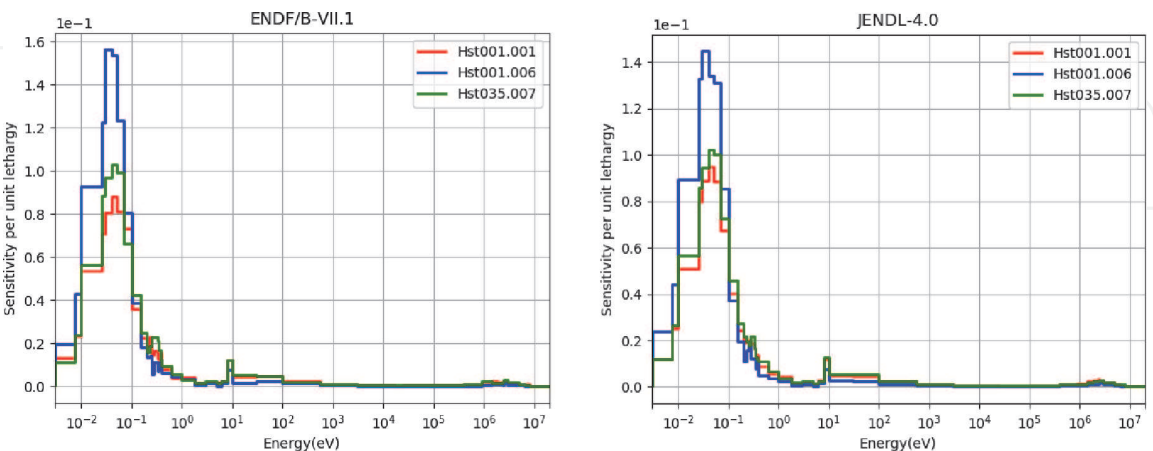


Figure 10.
Sensitivity profiles of ^{235}U fission cross section for thermal benchmarks with 44 energy groups—ENDF/B-VII.1 and JENDL-4.0.

3.3 Sensitivities of k_{eff} with respect to multigroup cross section

In this study, the sensitivity coefficients obtained with the two libraries ENDF/B-VII.1 and JENDL-4.0 are evaluated using MCNP6.1 code in three

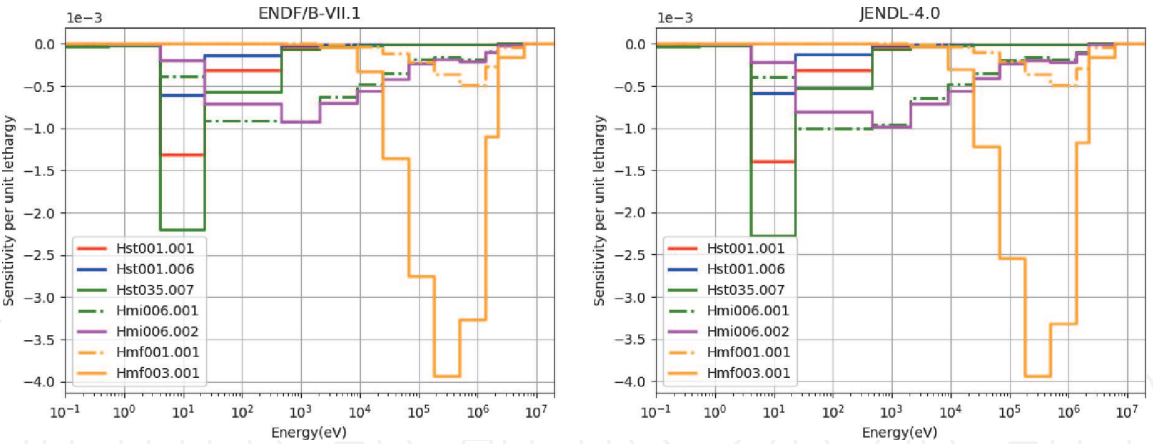


Figure 11.
Sensitivity profiles of the ^{238}U capture cross section with 15 energy groups—ENDF/B-VII.1 and JENDL-4.0.

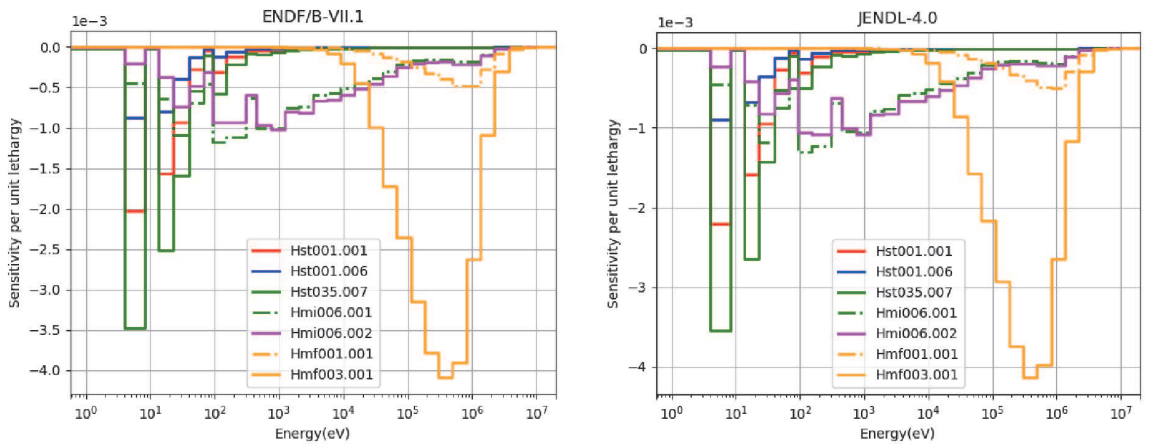


Figure 12.
Sensitivity profiles of the ^{238}U capture cross section with 33 energy groups—ENDF/B-VII.1 and JENDL-4.0.

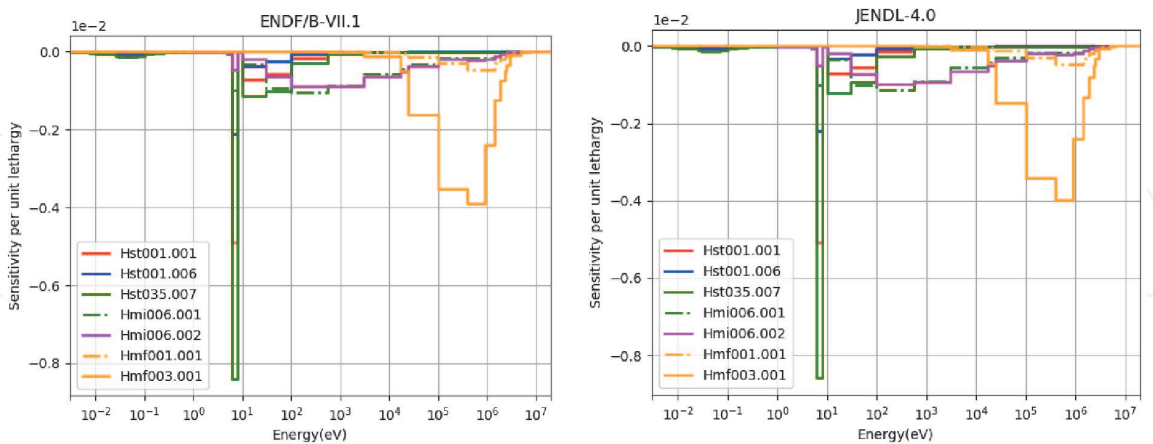


Figure 13.
Sensitivity profiles of the ^{238}U capture cross section with 44 energy groups—ENDF/B-VII.1 and JENDL-4.0.

multigroup structures (15, 33, and 44). Given the large number of cross sections for each energy group, the sensitivities of certain cross sections are only presented.

3.3.1 Sensitivity for the ^{235}U cross section

The results obtained are presented in the figures below for the ^{235}U cross sections (Figures 5–10).

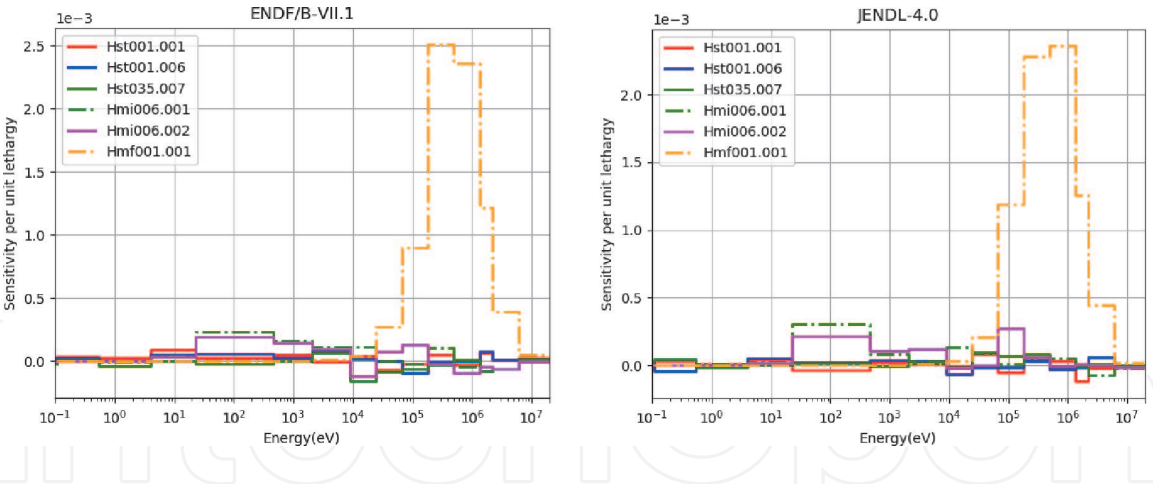


Figure 14.
Sensitivity profiles of the ^{238}U elastic cross section with 15 energy groups—ENDF/B-VII.1 and JENDL-4.0.

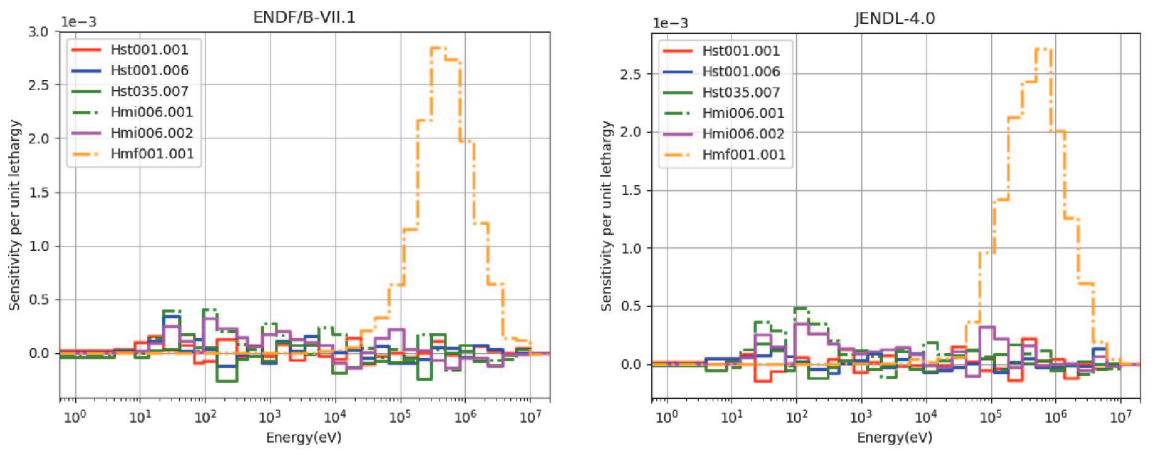


Figure 15.
Sensitivity profiles of the ^{238}U elastic cross section with 33 energy groups—ENDF and JENDL-4.0.

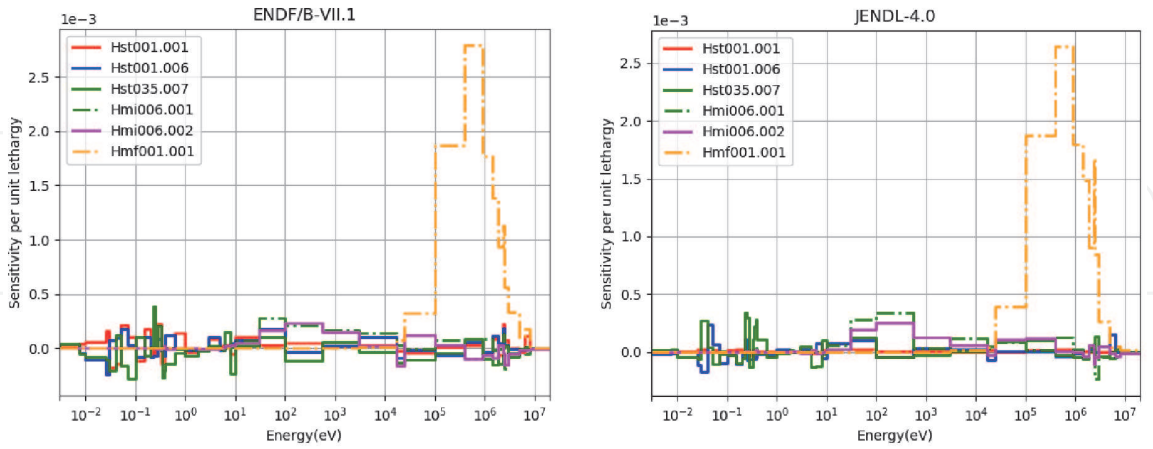


Figure 16.
Sensitivity profiles of the ^{238}U elastic cross section with 44 energy groups—ENDF and JENDL-4.0.

From these figures, it can be seen that the 44-group structure of energy gives very varied sensitivity profiles depending on the neutron energy; moreover, this group structure gives sensitivities slightly lower than those given by the structures of 15 and 33 groups. Consequently, it can be said that the precision of the sensitivity increases for the structure containing the largest number of energy groups. Thus, low uncertainties on nuclear data are expected with this structure (44 groups) in the two evaluations (ENDF/B-VII.1 and JENDL-4.0).

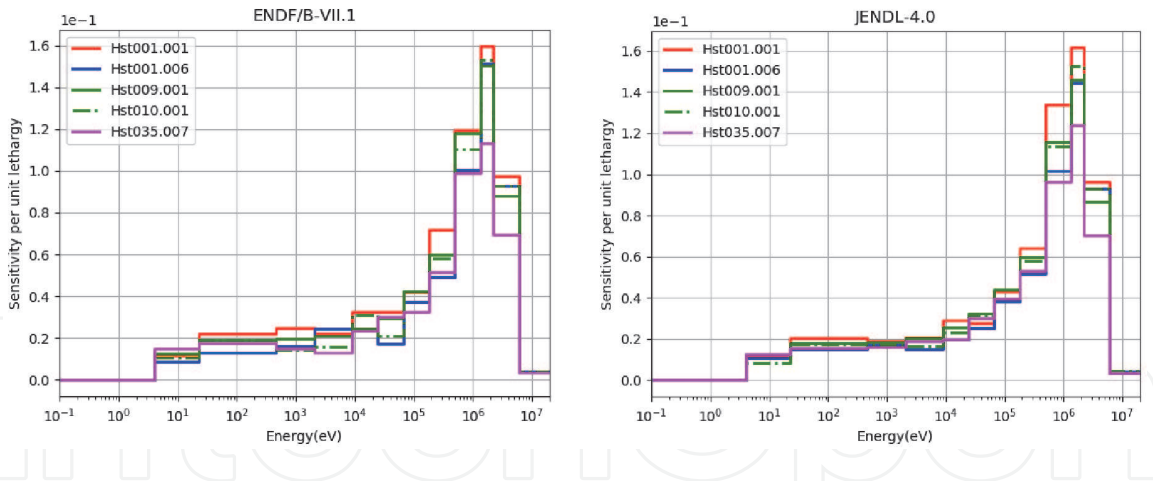


Figure 17.
Sensitivity profiles of the ^1H elastic cross section with 15 energy groups—ENDF/B-VII.1 and JENDL-4.0.

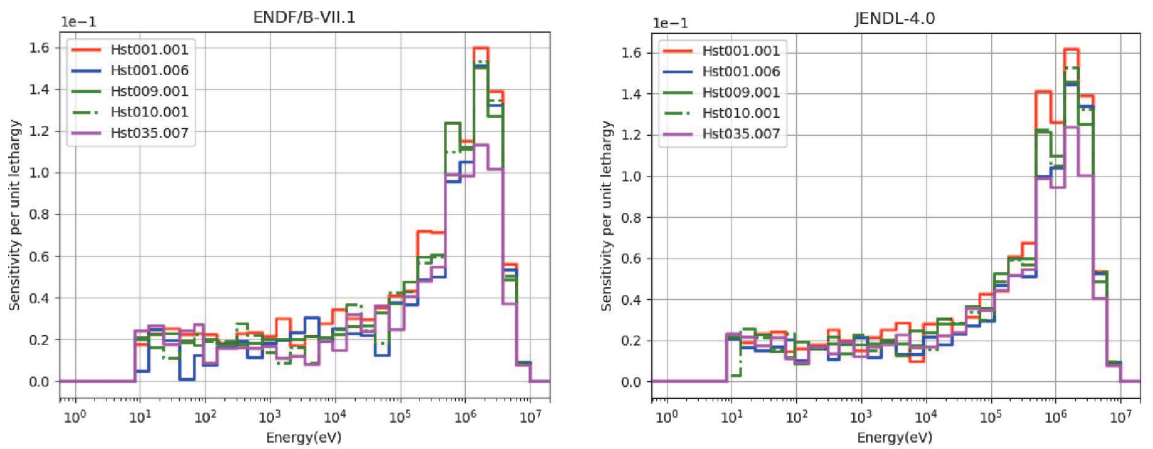


Figure 18.
Sensitivity profiles of the ^1H elastic cross section with 33 energy groups—ENDF/B-VII.1 and JENDL-4.0.

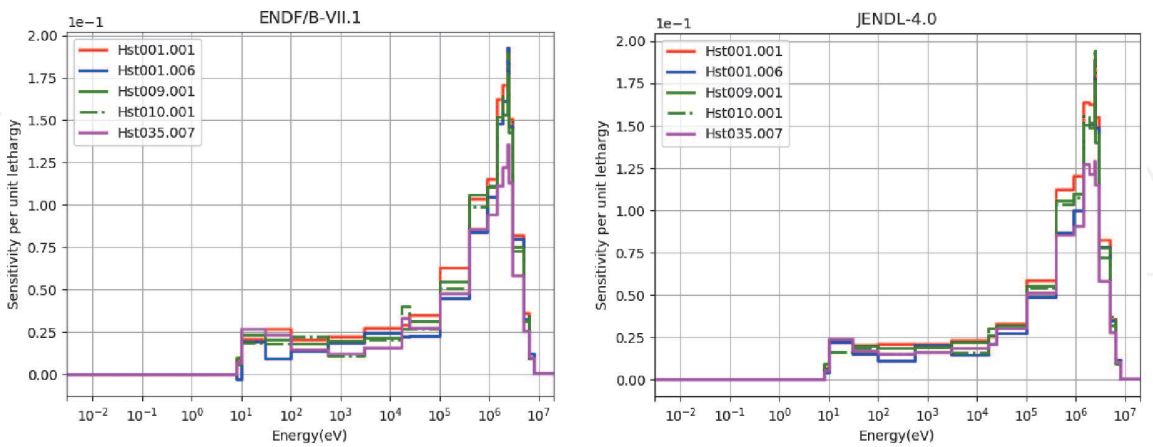


Figure 19.
Sensitivity profiles of the ^1H elastic cross section with 44 energy groups—ENDF/B-VII.1 and JENDL-4.0.

3.3.2 Sensitivity for the ^{238}U cross section

The sensitivities of the multiplication factors for the ^{238}U cross sections are shown in the figures below (**Figures 11–16**).

These figures show that thermal and intermediate critical experiment designs demonstrate low sensitivity to the capture and elastic cross sections of the ^{238}U at

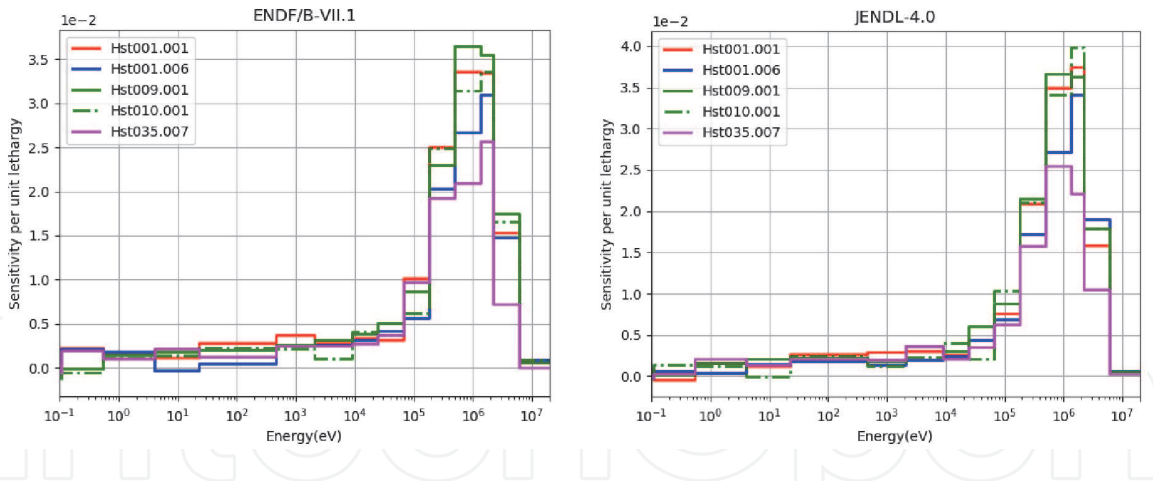


Figure 20.
Sensitivity profiles of the ^{16}O elastic cross section with 15 energy groups—ENDF/B-VII.1 and JENDL-4.0.

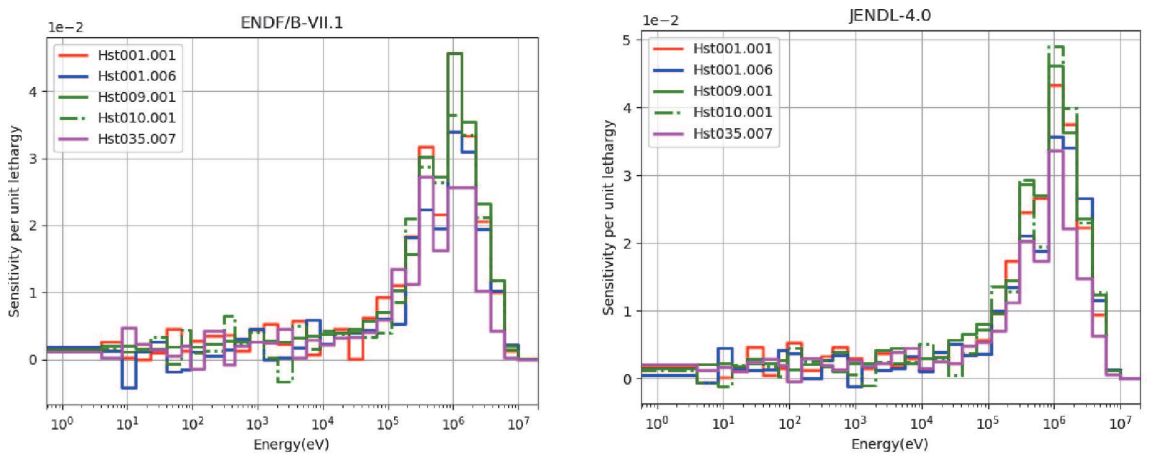


Figure 21.
Sensitivity profiles of the ^{16}O elastic cross section with 33 energy groups—ENDF/B-VII.1 and JENDL-4.0.

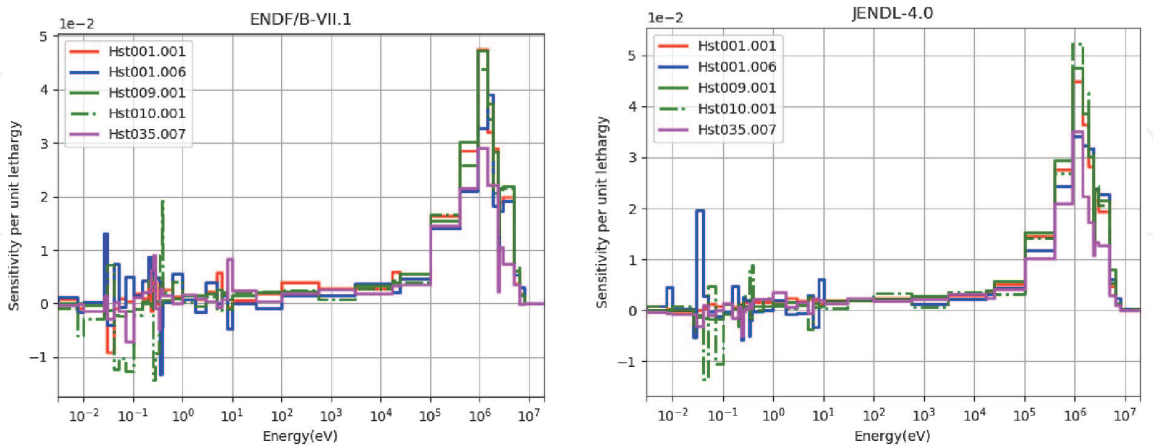


Figure 22.
Sensitivity profiles of the ^{16}O elastic cross section with 44 energy groups—ENDF/B-VII.1 and JENDL-4.0.

high energies and a significant sensitivity at thermal and resonance energies. However, the fast critical experiments demonstrate, at high energies, high levels of sensitivity to the capture and elastic cross sections of the ^{238}U . Also, the structure of the 44 energy groups gives very varied sensitivity profiles compared to those given by structures 15 and 33.

3.3.3 Sensitivity for ^1H and ^{16}O cross sections

The sensitivities of the k_{eff} 's with respect to the cross sections of ^1H and ^{16}O are presented in the figures below (**Figures 17–22**).

The figures above show that all thermal critical benchmarks demonstrate low sensitivity to the ^1H and ^{16}O elastic cross sections for low resonance energies and significant sensitivity for high energies. In addition, the structure of the 44 energy groups gives very varied sensitivity profiles compared to those given by the 15- and 33-group structures. Also, the sensitivities given by ENDF/B-VII.1 are slightly lower than those given by JENDL-4.0.

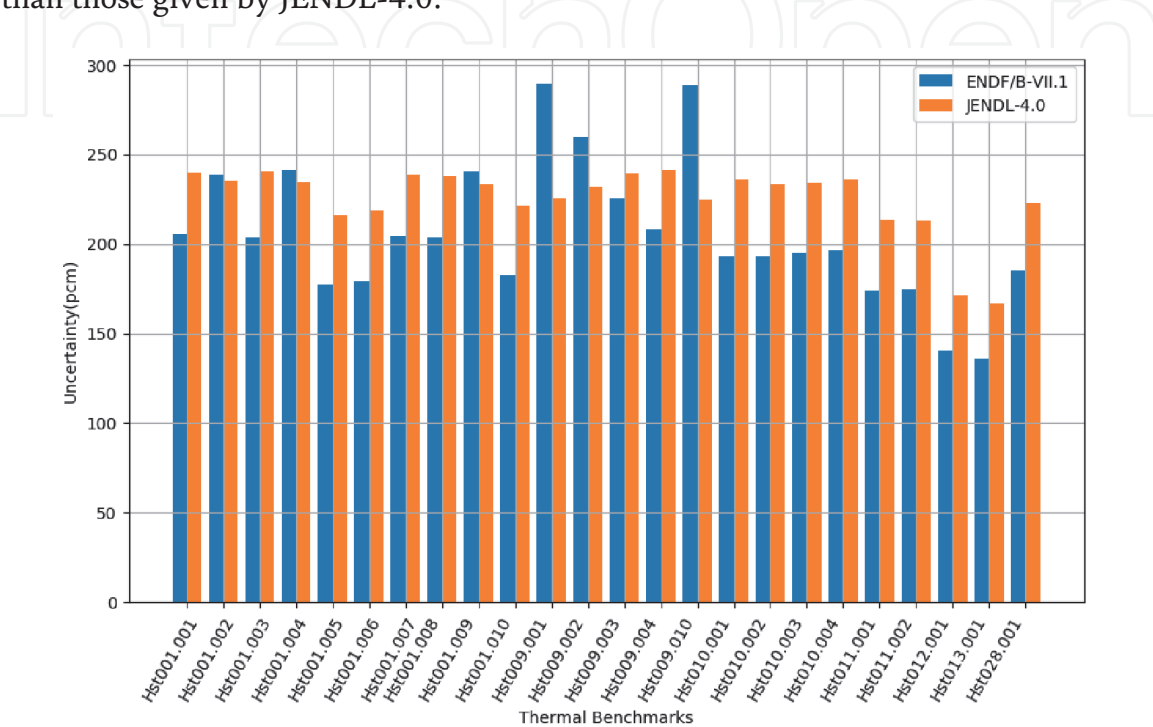


Figure 23. $\Delta k/k$ (pcm) prediction due to the uncertainties in ^{235}U capture cross sections with 44 energy groups for thermal benchmarks—ENDF/B-VII.1 and JENDL-4.0.

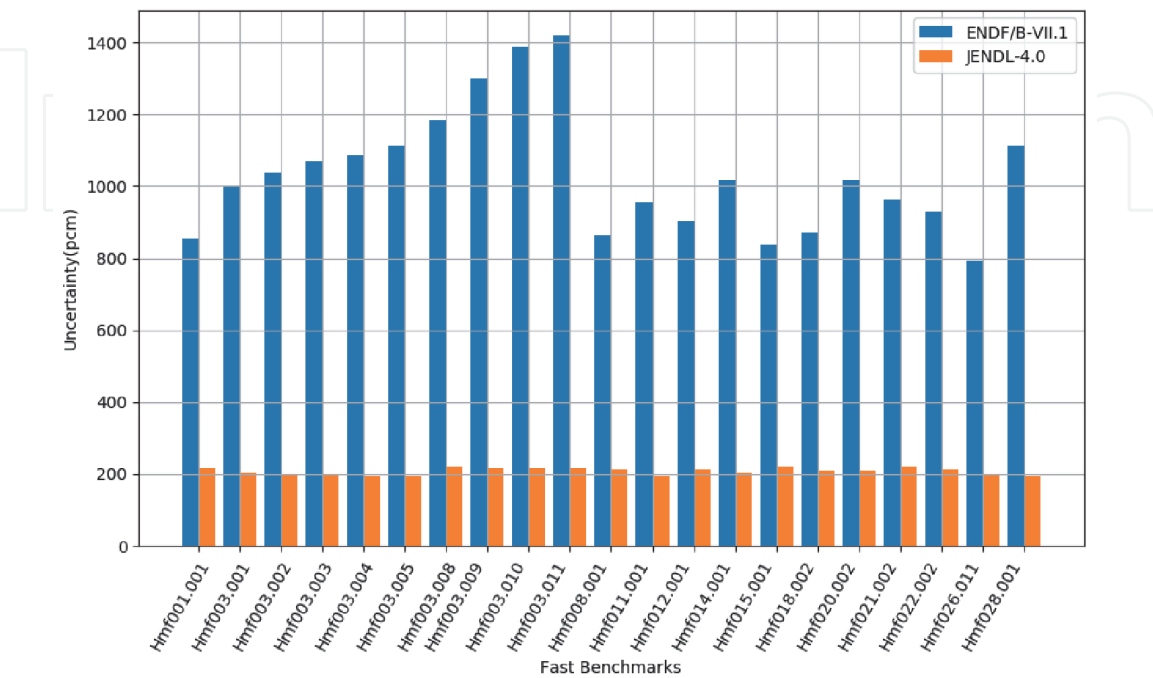


Figure 24. $\Delta k/k$ (pcm) prediction due to the uncertainties in ^{235}U capture cross sections with 44 energy groups for fast benchmarks—ENDF/B-VII.1 and JENDL-4.0.

In the following, all the results concerning only the structure of the group of 44 neutrons and presented for both ENDF/B-VII.1 and JENDL-4.0.

3.4 Nuclear data uncertainty prediction of k_{eff}

The nuclear data uncertainties of k_{eff} are calculated using Eq. (7), and the predictions of $\Delta k/k$ due to the uncertainty of the ^{235}U cross sections are presented in the figures below (Figures 23–26).

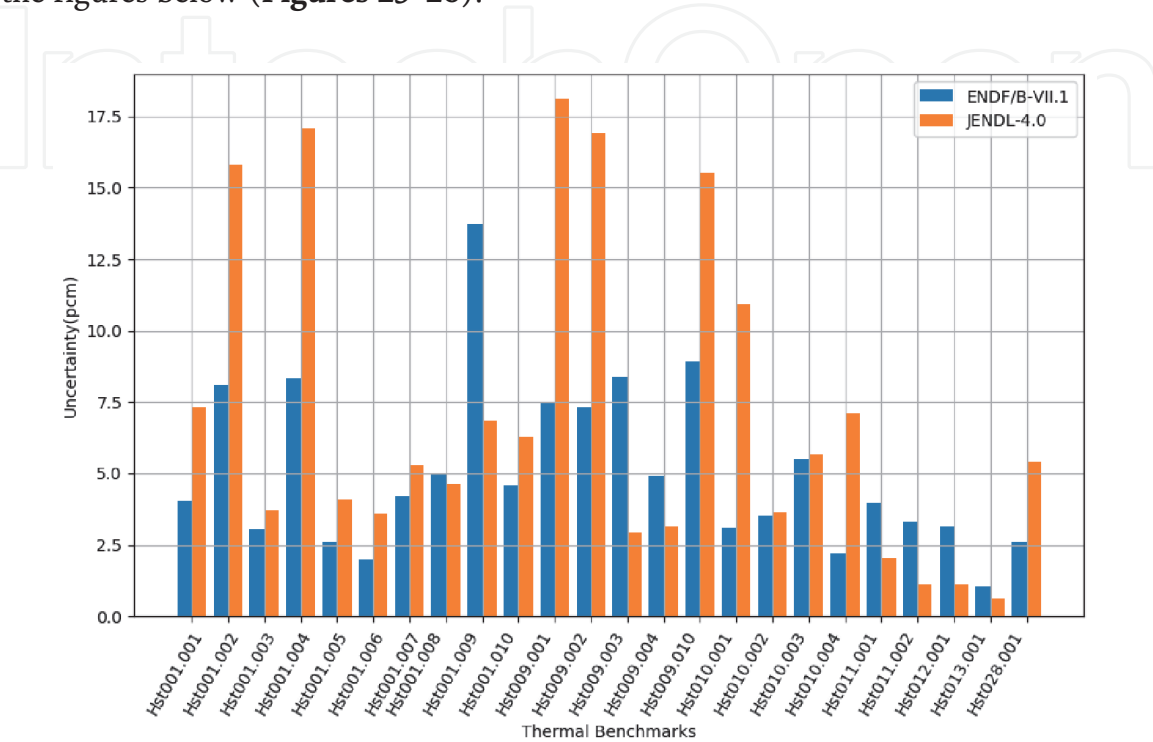


Figure 25. $\Delta k/k$ (pcm) prediction due to the uncertainties in ^{235}U elastic cross sections with 44 energy groups for thermal benchmarks—ENDF/B-VII.1 and JENDL-4.0.

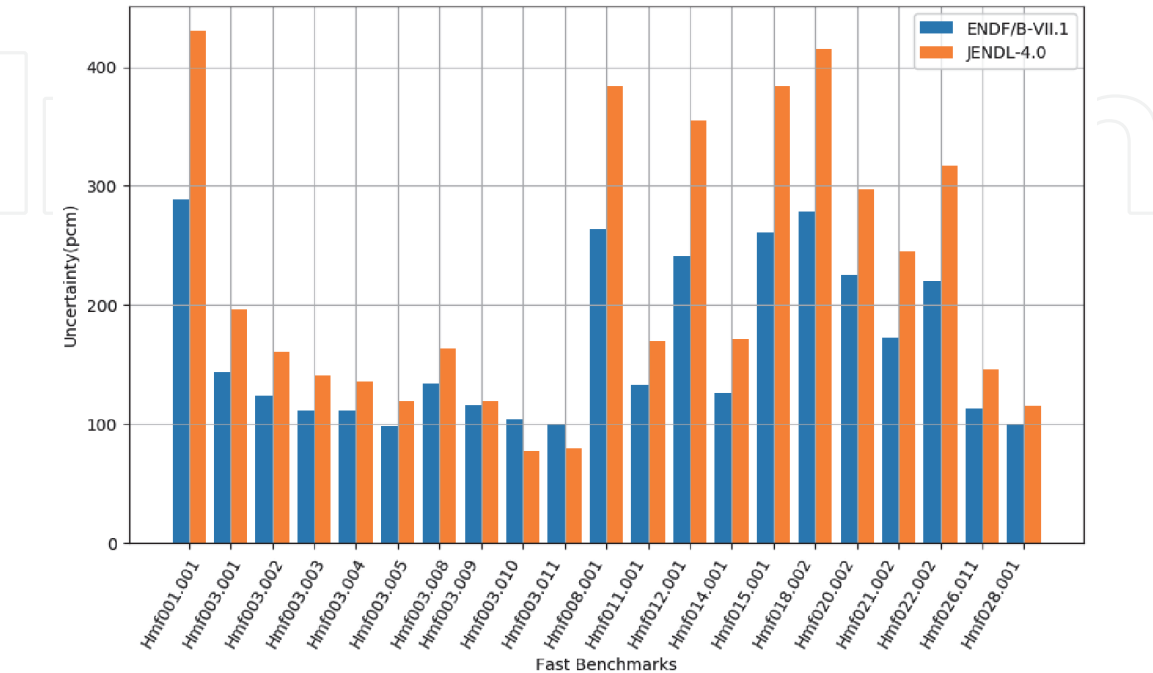


Figure 26. $\Delta k/k$ (pcm) prediction due to the uncertainties in ^{235}U elastic cross sections with 44 energy groups for fast benchmarks—ENDF/B-VII.1 and JENDL-4.0.

Thermal benchmarks	$\Delta k_{\text{eff}}/k_{\text{eff}}(\%)$ ENDF/B-VII.1	$\Delta k_{\text{eff}}/k_{\text{eff}}(\%)$ JENDL-4.0	Fast benchmarks	$\Delta k_{\text{eff}}/k_{\text{eff}}(\%)$ ENDF/B-VII.1	$\Delta k_{\text{eff}}/k_{\text{eff}}(\%)$ JENDL-4.0
Hst001.001	0.962	1.564	Hmi006.001	0.617	0.389
Hst001.002	0.931	1.214	Hmi006.002	0.800	0.274
Hst001.003	0.963	1.566	Hmi006.003	0.628	0.143
Hst001.004	0.934	1.200	Hmi006.004	0.827	0.159
Hst001.005	1.021	2.219	Hmf001.001	0.439	0.063
Hst001.006	1.011	2.160	Hmf003.001	0.442	0.057
Hst001.007	0.965	1.609	Hmf003.002	0.490	0.075
Hst001.008	0.963	1.587	Hmf003.003	0.492	0.083
Hst001.009	0.940	1.227	Hmf003.004	0.598	0.129
Hst001.010	0.995	2.104	Hmf003.005	0.446	0.053
Hst009.001	0.918	1.051	Hmf003.008	0.702	0.189
Hst009.002	0.929	1.122	Hmf003.009	0.667	0.159
Hst009.003	0.947	1.281	hmf003.010	0.603	0.141
Hst009.004	0.980	1.471	Hmf003.011	0.543	0.096
Hst009.010	0.917	1.065	Hmf008.001	0.648	0.221
Hst010.001	1.004	1.785	Hmf011.001	0.505	0.999
Hst010.002	1.009	1.820	Hmf012.001	0.458	0.086
Hst010.003	1.004	1.800	Hmf014.001	0.462	0.070
Hst010.004	1.010	1.747	Hmf015.001	0.463	0.084
Hst011.001	1.069	2.295	Hmf018.002	0.437	0.057
Hst011.002	1.074	2.306	Hmf020.002	0.447	0.244
Hst012.001	1.274	3.150	Hmf021.002	0.423	0.035
Hst013.001	1.281	3.237	Hmf022.002	0.421	0.035
Hst028.001	1.007	2.066	Hmf026.011	0.505	1.326
Hst035.007	0.880	1.682	Hmf028.001	0.489	0.075

Table 7.
Total uncertainty of k_{eff} (%).

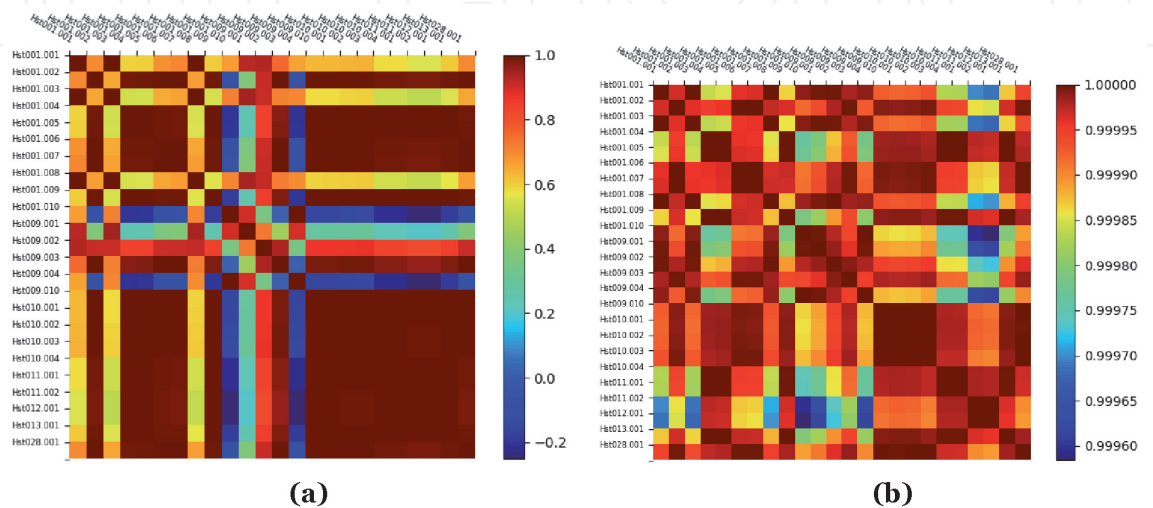


Figure 27.
Correlation between thermal benchmarks due to the uncertainties in ^{235}U capture cross sections. (a) ENDF/B-VII.1 (b) JENDL-4.0.

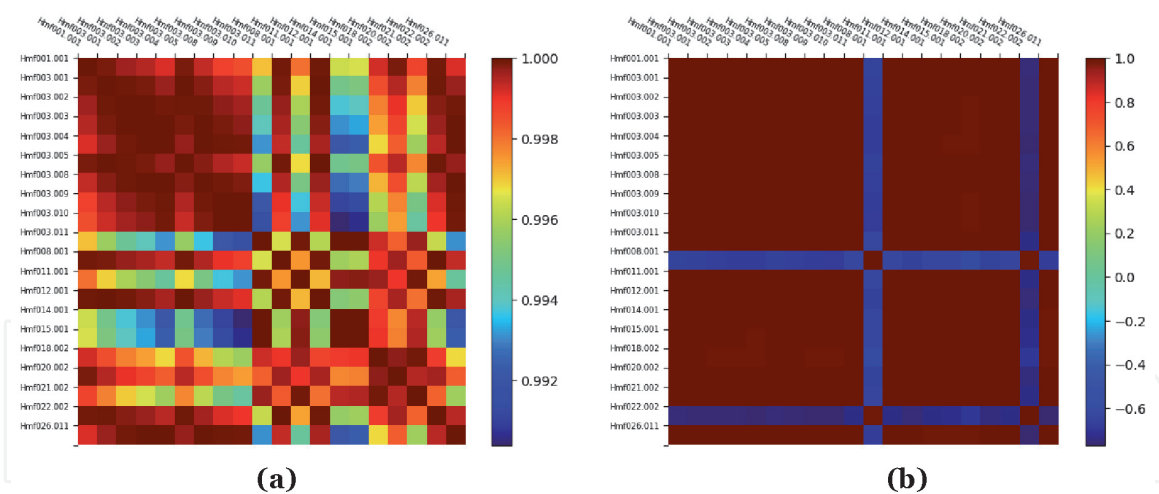


Figure 28.
Correlation between fast benchmarks due to the uncertainties in ^1H and ^{16}O capture and elastic cross sections.
(a) ENDF/B-VII.1 (b) JENDL-4.0.

We can see from these figures that, in general, the relative uncertainties of k_{eff} using ENDF/B-VII.1 are less than those using JENDL-4.0. For example, these uncertainties due to the ^{235}U capture cross section are ~ 250 pcm, and in the elastic cross section case, they are ~ 15 pcm for thermal benchmarks and 100–400 pcm for fast benchmarks. Concerning the predictions $\Delta k/k$ due to the uncertainty of the ^{238}U cross sections, they are all very small except for the elastic and inelastic cross sections.

The total uncertainties of the effective multiplication factors due to U-235, U-238, H-1, and O-16 are summarized in **Table 7**.

Table 7 shows that for thermal benchmarks, the relative uncertainties of k_{eff} with the ENDF/B-VII.1 are lower than those with JENDL-4.0. However, for fast benchmarks, these uncertainties are greater with the JENDL-4.0 evaluation.

3.5 Correlation between benchmark errors

The degree of correlation between benchmarks errors is calculated using Eq. (6); the results obtained are presented in the figures below.

Figures 27 and 28 show that the correlations between the benchmarks using ENDF/B-VII.1 are lower than those using JENDL-4.0. Thus, a close similarity between several experiences is noted.

4. Conclusions

The multigroup effect on the sensitivities of k_{eff} with respect to cross sections U-235, U-238, H-1, and O-16 is studied using 15, 33, and 44 energy groups. We found that the structure of the 44 groups gives the most varied sensitivity profiles in the two evaluations ENDF/B-VII.1 and JENDL-4.0, allowing a better investigation of the uncertainties of the nuclear data.

The results obtained show that the k_{eff} sensitivity profiles are approximately the same for the two nuclear evaluations ENDF/B-VII.1 and JENDL-4.0. However, the covariances of the cross sections are different between the two evaluations, which is why differences between the uncertainties of the nuclear data are observed between these evaluations. For example, the total uncertainties in the thermal benchmark Hst001.001 are, respectively, 0.962 and 1.564% with ENDF/B-VII.1 and JENDL-4.0, and for the fast benchmark Hmf.001.001, these uncertainties are 0.439 and

0.063% with ENDF/B -VII.1 and JENDL-4.0, respectively. These differences are mainly due to the high covariances in JENDL-4.0 compared to those in ENDF/B-VII.1, in particular for the elastic cross section of the U-235 and of the fission for the U-238.

These results demonstrated that the covariances of most neutron reactions with the nuclei studied in this work require more investigation and re-estimation.

Acknowledgements

The work leading to this publication has been supported by the Radiations and Nuclear Systems Laboratory at Abdelmalek Essaadi University of Tetuan. Thank you to all the contributors of our laboratory team.

Author details


Mustapha Makhloul^{1*}, H. Boukhal¹, T. El Bardouni¹, E. Chakir², M. Kaddour¹ and S. Elouahdani¹

¹ Radiations and Nuclear Systems Laboratory, Faculty of Sciences of Tetuan, University Abdelmalek Essaadi, Morocco

² SIMO Lab, Faculty of Sciences of Kenitra, Morocco

*Address all correspondence to: mustapha342011@hotmail.fr

IntechOpen

© 2020 The Author(s). Licensee IntechOpen. This chapter is distributed under the terms of the Creative Commons Attribution License (<http://creativecommons.org/licenses/by/3.0>), which permits unrestricted use, distribution, and reproduction in any medium, provided the original work is properly cited. 

References

- [1] Cabellos O. Presentation and discussion of the UAM/exercise I-1b: "Pin-cell burn-up benchmark" with the hybrid method. Science and Technology of Nuclear Installations. 2013;2013:1-12. DOI: 10.1155/2013/790206
- [2] Vibha V, Mukherjee S, Naik H, Parashari S, Makwana R, Suryanarayana SV. $^{238}\text{U}(n,\gamma)$ Reaction Cross-Section at the Neutron Energy 8.96 MeV; 2017
- [3] Iwamoto O et al. Uranium-235 Capture Cross-Section in the keV to MeV Energy Region; 2011
- [4] Palmiotti G et al. Combined use of integral experiments and covariance data. Nuclear Data Sheets. 2014;118: 596-636. DOI: 10.1016/j.nds.2014.04.145
- [5] Otuka N, Nakagawa T, Shibata K. Uranium-235 neutron capture cross section at keV energies. Journal of Nuclear Science and Technology. 2007; 44(6):815-818. DOI: 10.1080/18811248.2007.9711318
- [6] Pelowitz DB et al. MCNP6 User's Manual. Los Alamos National Laboratory; 2013
- [7] Macfarlane RE, Muir DW, Boicourt RM, Kahler AC. The NJOY Nuclear Data Processing System, Version 2012. Los Alamos National Laboratory (LANL); 2012
- [8] Briggs JB. International handbook of evaluated criticality safety benchmark experiments. Nuclear Energy Agency, NEA/NSC/DOC (95). Exp. Needs Crit. Saf., vol. 3, Sep. 2004 [Online]. Available: <https://www.oecd-neo.org/science/wpncs/icsbep/handbook.html>
- [9] Kaddour M. Analyse de sensibilité des problèmes de criticité et du coefficient de température aux données nucléaires: Contribution à l'amélioration des évaluations des sections efficaces et application à une maquette critique: le réacteur expérimentale EOLE; 2015
- [10] Bowman SM. Experience with the SCALE Criticality Safety Cross-Section Libraries. Washington, DC: The Office: For sale by the U.S. G.P.O., Supt. of Docs.; 2000
- [11] Broadhead BL, Rearden BT, Hopper CM, Wagschal JJ, Parks CV. Sensitivity and uncertainty based criticality safety validation techniques. Nuclear Science and Engineering. 2004; 146(3):340-366
- [12] Rochman D, Vasiliev A, Ferroukhi H, Zhu T, van der Marck SC, Koning AJ. Nuclear data uncertainty for criticality-safety: Monte Carlo vs. linear perturbation. Annals of Nuclear Energy. 2016;92:150-160. DOI: 10.1016/j.anucene.2016.01.042
- [13] Sobes V, Leal L, Arbanas G, Forget B. Resonance parameter adjustment based on integral experiments. Nuclear Science and Engineering. 2016;183(3). DOI: 10.13182/NSE15-50
- [14] Kiedrowski BC. 'MCNP6. 1 k-Eigenvalue sensitivity capability: a user's guide', Los Alamos National Laboratory (LANL), MCNP Documentation & Website; 2013. DOI: 10.13182/NSE10-22
- [15] Chow ETY. An investigation of methods for neutron cross section error identification utilizing integral data [PhD thesis]. Georgia Institute of Technology; 1974
- [16] Reupke WA. The consistency of differential and integral thermonuclear neutronics data [PhD thesis]. Georgia Institute of Technology; 1977
- [17] Williams ML, Wiarda D, Ilas G, Marshall WJ, Rearden BT. Covariance

applications in criticality safety, light water reactor analysis, and spent fuel characterization. Nuclear Data Sheets. 2015;**123**:92-96

[18] Broadhead B, Hopper CM, Parks CV, Childs RL. Sensitivity and Uncertainty Analyses Applied to Criticality Safety Validation, methods development. United States: Oak Ridge National Lab; ORNL/TM-13692/V1. 1999

[19] Kuroi H, Mitani H. Adjustment to cross section data to fit integral experiments by least squares method. Journal of Nuclear Science and Technology. 1975;**12**(11):663-680

[20] Makhloul M, Boukhal H, El Bardouni T, Kaddour M, Chakir E, El Ouahdani S. ^{235}U elastic cross-section adjustment in criticality benchmarks – Comparison between JENDL-4.0 and ENDF/-VII.1. Annals of Nuclear Energy. 2018;**114**:541-550. DOI: 10.1016/j.anucene.2017.12.018

[21] Salvatores M et al. Methods and issues for the combined use of integral experiments and covariance data: Results of a NEA international collaborative study. Nuclear Data Sheets. 2014;**118**:38-71